IOP Publishing Superconductor Science and Technology
Supercond. Sci. Technol. 31 (2018) 085008 (9pp) https://doi.org/10.1088/1361-6668/aad080

Novel configuration of a HTS filter with adjustable transmission zeros based on a modified cascaded quartet structure

Liguo Zhou, Hui Li, Zhihe Long, Hang Wu, Tianliang Zhang and Man Qiao

School of Aeronautics and Astronautics, University of Electronic Science and Technology of China, Chengdu 611731, People's Republic of China

E-mail: ztl@uestc.edu.cn

Received 8 April 2018, revised 29 June 2018
Accepted for publication 2 July 2018
Published 17 July 2018

Abstract

A novel configuration for adjusting the relative position of transmission zeros (TZs) based on the cascaded quartet (CQ) structure filter is proposed. By simply introducing joint cross coupling (JCC) between two adjacent CQ units of the filter and changing its coupling strength, the relative position of TZs produced by the conventional CQ units can be altered easily so as to achieve better selectivity and out-of-band rejection. The filter with the proposed configuration is named a quasi-CQ (QCQ) configuration filter in this paper. The symmetrical QCQ configuration filter can obtain the frequency response of the asymmetrical filter, so the design difficulty of filters with multiple pairs of separated TZs is greatly reduced. A series of prototypes of QCQ configuration filters is given and analyzed to provide design guidance for designers in the future. Finally, the correctness and feasibility of the proposed approach are verified by fabricating and measuring a symmetrical high-temperature superconducting QCQ configuration filter, and the test results accord well with the simulated ones.

Keywords: cascaded quartet (CQ), filter, high-temperature superconducting (HTS), joint cross coupling, TZs

(Some figures may appear in colour only in the online journal)

1. Introduction

The rapid development of wireless communications presents an urgent demand for high-performance radio frequency/microwave bandpass filters. Filters with advantages such as low insertion loss, a high-quality factor and excellent out-of-band rejection are widely researched by scholars [1–10]. In order to obtain a better selectivity within a limited area of high-temperature superconducting (HTS) thin films, introducing cross coupling between non-adjacent resonators [11–17], adopting parallel topology [18–20] and extracted-pole technology [18–24] to realize the quasi-elliptic function [13–17, 25–37] and generalized Chebyshev function [38–41] filters for producing transmission zeros (TZs) at finite frequencies are common approaches; most especially, quasi-elliptic function filters with cross-coupled folded configurations which can introduce pairs of TZs are increasingly prevalent [13–17, 28–38, 41, 42]. This is because the effect of each crossing-coupling section on the performance of the filter with cross-coupled folded configurations is relatively independent, and it is also convenient for designing and tuning. There are various cross-coupled folded configurations shown in figure 1, such as the inline topology, Pfitzenmaier configuration [39], cascaded quartet (CQ) configuration [13, 17, 26–35], cul-de-sac configuration [39] and parallel-connected configuration [42–44]. The solid black dots and the nearby numbers represent the resonators and their numbers, respectively, and S (source) and L (load) respectively indicate the input and output ports in figure 1.

Among them, the CQ structure is the most commonly-used. In [13–17, 25–34, 36–39], filters with high selectivity are all realized by using several CQ units, which could greatly

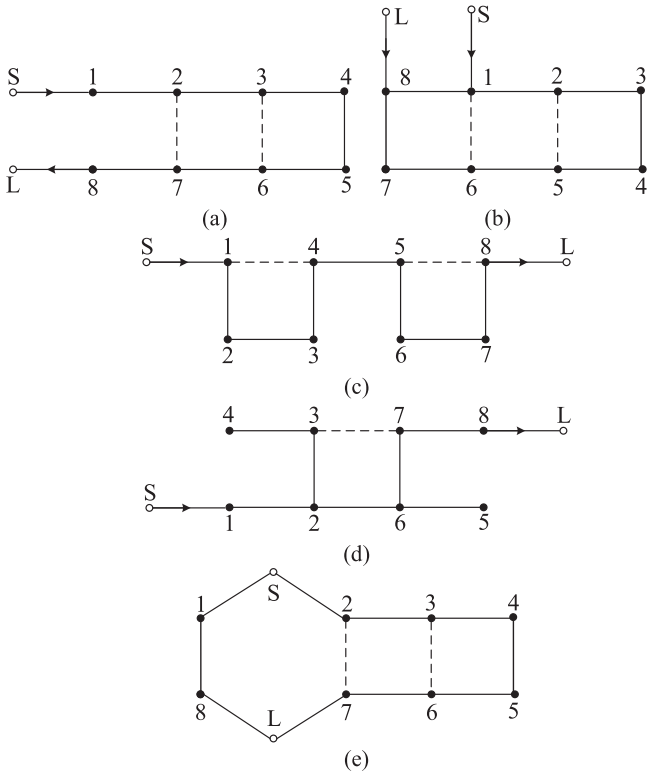

Figure 1. Cross-coupled folded configurations of filter: (a) inline topology, (b) Pfitzenmaier configuration, (c) CQ configuration, (d) cul-de-sac configuration, and (e) parallel-connected configuration.

improve out-of-band rejection. There are two kinds of frequently-used conventional structures when researchers design physical filters with CQ configuration: one is adding the cross-coupling line between non-adjacent resonators, like the CQ structure filters in [3, 12–14, 25, 30, 32, 33, 37], and the other is like those in [17, 26–31, 34–36], which are constructed by keeping four resonators near to each other (dual-row structure) to realize cross coupling. It is well known that a symmetrical filter is easier to design than a filter with an asymmetrical structure, especially for high-order passband filter design, because design variables will be halved and the speed of the optimization will be improved substantially. But if the CQ structure filters are symmetrical, the TZs generated by the CQ units will be overlapped. Obviously, if TZs are separated and located at different positions outside the passband, it will be more beneficial to the out-of-band rejection. However, for achieving the separation of TZs in order to obtain superior out-of-band rejection, asymmetrical structures are always employed [12, 13, 25–31, 34, 35], namely, the filter layout and the normalized coupling coefficient matrix are both asymmetrical, which means the difficulty of design is greatly increased. Take the 8-order filter topology in figure 2(a) for instance, where the small black point with a number indicates the resonator. The solid and dash line represent the direct coupling and cross coupling, respectively. Each CQ unit is comprised of four coupled resonators with a cross coupling. In order to prevent the two pairs of TZs generated by the two CQ units (left CQ unit and right CQ unit) overlapping, all the coupling coefficients in the left CQ

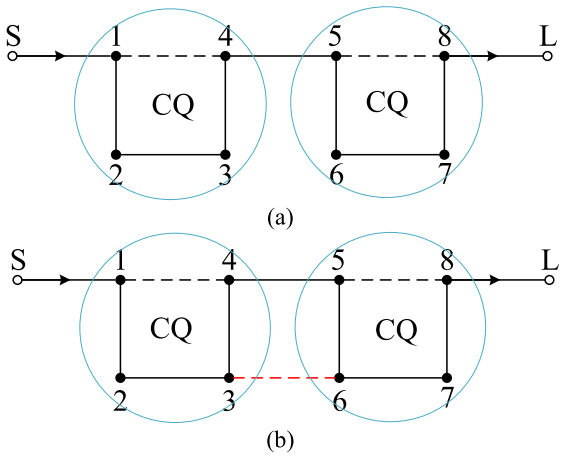

Figure 2. (a) Topology of 8-order conventional filter with two CQ units, (b) topology of 8-order quasi-CQ (QCQ) configuration filter.

unit are possibly different from those in the right one. So the tuning variables will double and the time spent on full-wave electromagnetic (EM) simulation will exponentially increase, compared with the design of symmetrical filters. Therefore, an approach which can simply realize the adjustment of TZs in symmetrical filters is very meaningful and attractive for reducing the workload of designers.

In this paper, a novel configuration is proposed for symmetrical filters to separate the overlapped TZs and adjust their relative distance by introducing joint cross coupling (JCC) between the two adjacent CQ units to form a QCQ unit; its topology is shown in figure 2(b). When JCC is introduced into the symmetrical filter, the overlapped TZs will be separated, which means the symmetrical filter can realize the frequency response of the asymmetrical one so as to meet the increasing demand of excellent out-of-band suppression. In order to illustrate and verify the proposed QCQ configuration better, the structure of this paper is planned as follows. In section 2, the coupling and routing diagrams of 8-order, 10-order and 12-order filters with one JCC and a 12-order filter with two JCCs are presented. Furthermore, considering an 8-order filter for example, the phase requirements that the QCQ configuration filter should satisfy are also given in this section. In section 3, the normalized prototype network of 8-order symmetrical structures, a 10-order symmetrical structure, and a 12-order filter with one JCC and two JCCs are analyzed. In section 4, according to the analyzed QCQ configuration filters above, an 8-order symmetrical HTS filter is designed by employing a flexible resonator structure, and the measured results agree rather well with the simulated ones.

2. Synthesis of filters with QCQ configuration

2.1. Construction of QCQ configuration filter

Figure 2(a) is the typical 8-order bandpass filter topology with two CQ units. An 8-order QCQ configuration filter topology is formed by adding a JCC (the red dashed line) between

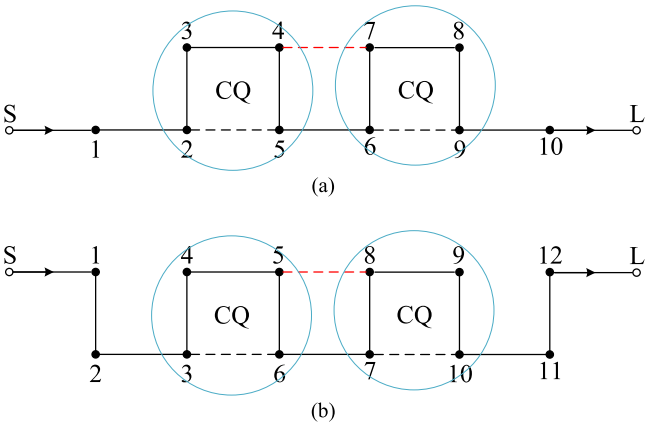

Figure 3. (a) Topology of 10-order QCQ configuration filter with two CQ units and a JCC, (b) 12-order QCQ configuration filter with two CQ units and a JCC.

resonators 3 and 6 of the two adjacent CQ units based on figure 2(a), as shown in figure 2(b).

Figure 3(a) shows the 10-order QCQ configuration filter topology with two CQ units and a JCC introduced between resonators 4 and 7. The 12-order QCQ configuration filter topology is presented in figure 3(b). In addition, a 12-order QCQ configuration filter with three CQ units and two JCCs is shown in figure 4. According to this rule, higher order filters with more CQ units and JCCs can also be constructed.

2.2. Phase analysis of 8-order QCQ configuration filter

In order to present the characteristics of arbitrary order symmetrical QCQ configuration filters, an 8-order filter is taken for an example in this subsection to analyze the phase and structure properties. Figure 5 is the general multipath coupling diagram of an 8-order QCQ configuration filter. The angle between the two resonators indicates the phase shift, and the positive and negative signs represent the electric field coupling and magnetic field coupling, respectively. Based on the phase theory of the filter, if the coupling between two resonators is the magnetic field coupling, the phase shift of the signal tends toward $-90°$, and if that is the electric field coupling, the phase shift of the signal tends toward $+90°$. On the other hand, for signals below the resonant frequency (below the passband) of resonators, the phase shift tends toward $+90°$. However, for those above resonance, the phase shift tends toward $-90°$. The theoretical analysis of phase shift has been studied in great detail in [15, 16, 19, 24]. Due to the various phase variations mentioned above, the 8-order filter has many kinds of phase shifts from input to output. Figure 5 gives all possible forms in the multipath coupling diagram. In addition, it is necessary to explain the theory of the phase change of the CQ unit. According to the theory of the CQ structure filter, if the phase difference of the main signal path ① → ② → ③ → ④ (⑤ → ⑥ → ⑦ → ⑧) and the cross-coupling signal path ① → ④ (⑤ → ⑧) is 180° (out of phase), then a pair of TZs can be introduced outside the passband.

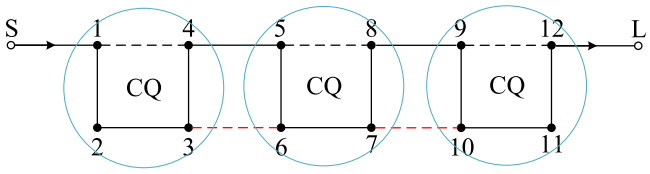

Figure 4. Topology of 12-order QCQ configuration filter with three CQ units and two JCCs.

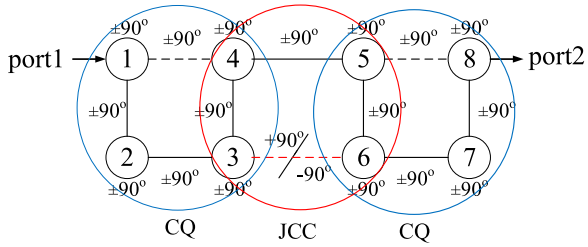

Figure 5. General multipath coupling diagram for 8-order QCQ configuration filter.

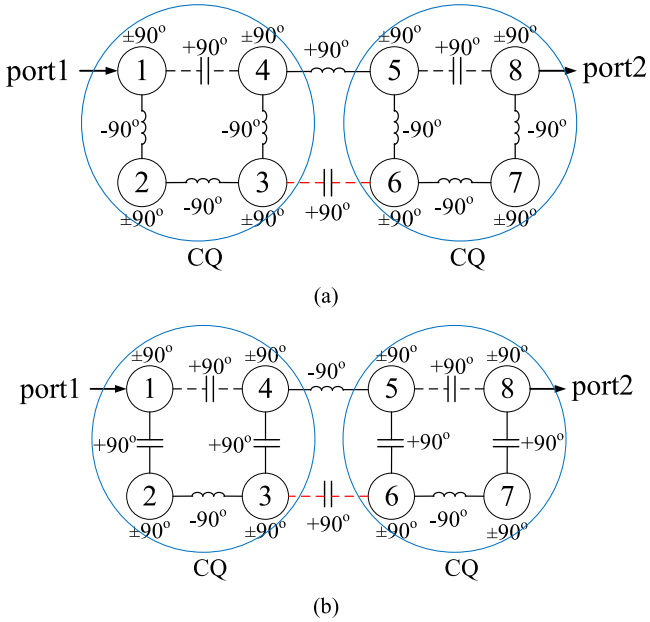

Figure 6. Two kinds of multipath coupling diagram of the 8-order QCQ configuration filter: (a) QCQ configuration filters type I, and (b) QCQ configuration filters type II.

In figure 5, as long as the two adjacent CQ units can separately produce a pair of TZs, and the coupling property of the JCC is opposite to that between resonators 4 and 5, the QCQ configuration filter can be realized. Therefore, many possible forms of the 8-order QCQ configuration filter exist, and figure 6 exhibits two of them.

After the introduction of the phase and structure properties in the 8-order filter, the TZs' adjustment characteristics of arbitrary order symmetrical QCQ configuration filters are summarized in table 1.

According to the topologies of the QCQ configuration filters in section 2.1 of section 2, the normalized coupling coefficient matrices are synthesized in sections 2.2 and 2.3 to provide theoretical guidance for the design of QCQ

Table 1. Characteristics of the symmetrical QCQ configuration filters.

Structure of filter	Phase difference	$\lvert m_{JCC}\rvert$	$\Delta\omega'$
Symmetrical	Out of phase	Increase	Increase from zero

Phase difference: the phase difference of signal paths in the JCC unit, such as the phase difference between signal paths ③ → ④ → ⑤ → ⑥ and ③ → ⑥ in the JCC unit of the 8-order filter in figure 6(a). $\lvert m_{JCC}\rvert$: coupling strength of JCC. $\Delta\omega'$: relative distance between two pairs of TZs, as shown in figure 7(a).

Table 2. The normalized coupling coefficient matrix of the 8-order symmetrical QCQ configuration filter.

	S	1	2	3	4	5	6	7	8	L
S	0	0	0	0	0	0	0	0	0	0
1	0	0	0.765	0	−0.170	0	0	0	0	0
2	0	0.765	0	0.674	0	0	0	0	0	0
3	0	0	0.674	0	0.497	0	$m_{3,6}$	0	0	0
4	0	−0.170	0	0.497	0	−0.519	0	0	0	0
5	0	0	0	0	−0.519	0	0.497	0	−0.170	0
6	0	0	0	$m_{3,6}$	0	0.497	0	0.674	0	0
7	0	0	0	0	0	0	0.674	0	0.765	0
8	0	0	0	0	0	−0.170	0	0.765	0	0
L	0	0	0	0	0	0	0	0	0	0

configuration filters. The corresponding normalized frequency responses are also presented to exhibit the control of TZs.

2.3. The analysis of 8-order symmetrical QCQ filters

According to the topology in figure 2(b), a set of 8-order symmetrical QCQ configuration filter self-synthesized normalized coupling coefficients is listed in table 2. $m_{i,j}$ represents the coupling coefficient between resonators i and j. The frequency responses with varied coupling strengths of JCC ($\lvert m_{3,6}\rvert$) of table 2 are shown in figure 7(a). It can be observed that when $m_{3,6}$ is equal to zero, the two pairs of TZs are overlapped, and with the increase of $m_{3,6}$ from 0 to 0.022, the normalized relative distance ($\Delta\omega'$) between them increases from zero. Therefore, by simply adjusting $m_{3,6}$, the two pairs of TZs can be altered simultaneously so as to satisfy the required out-of-band rejection.

It is obvious that when $m_{3,6}$ is changed, the other normalized coupling coefficients will vary as well, which will have an adverse impact on the return loss in the passband. Figure 7(b) shows the changes of the in-band voltage standing wave ratio (VSWR) and $\Delta\omega'/\omega_c'$ with varied $m_{3,6}$, where ω_c' is the normalized cut-off angular frequency. It can be observed that when $m_{3,6}$ varies from 0 to 0.03, $\Delta\omega'/\omega_c'$ climbs from 0 to 0.5% with VSWR within the passband changing slightly from 1.20 to 1.40. Thus by adjusting the coupling strength of JCC in the QCQ configuration filter, the frequency response of the symmetrical filter with separated and controllable TZs can be realized, which greatly simplifies the design difficulty of the 8-order CQ structure filter with two pairs of separated TZs.

2.4. Analysis of the high-order symmetrical QCQ configuration filter

According to the topologies in figures 3(a) and (b), two sets of symmetrical high-order filter self-synthesized normalized coupling matrices are listed in tables 3 and 4. Figures 8 and 9 show the corresponding prototype frequency responses of the 10-order filter with two CQ units and one JCC ($m_{4,7}$ is equal to 0, 0.011 and 0.022, respectively) using the normalized coupling matrix in table 3 and the 12-order filter with two CQ units and one JCC ($m_{5,8}$ is equal to 0, 0.011 and 0.022, respectively) using the normalized coupling matrix in table 4, under the case of the other coupling coefficients keeping unchanged. It can be observed from these two figures that when the filter structure is symmetrical and the phase difference between the main signal path and cross-coupling signal path in the JCC unit is 180° (out of phase), the relative distance between the two pairs of TZs increases from zero with the increase of the coupling strength of the JCC ($\lvert m_{JCC}\rvert$), which conforms to the rules proposed in table 1.

Figure 10 shows the prototype frequency responses of the 12-order symmetrical filter with three CQ units and two JCCs ($m_{3,6} = m_{7,10} = m_{c,c}$ are equal to 0, 0.011 and 0.022, respectively) in figure 4 using the normalized coupling coefficient matrix in table 5. It can be seen that there are only two pairs of TZs when $m_{c,c}$ are equal to zero, because the two pairs of TZs generated by CQ units are overlapped. And with the increase of $m_{c,c}$, the overlapped TZs are separated and the relative distance between them increases gradually, so there are three pairs of TZs later.

Therefore, it can be speculated that a higher order filter with more CQ units and JCCs satisfies the rules in table 1 as well.

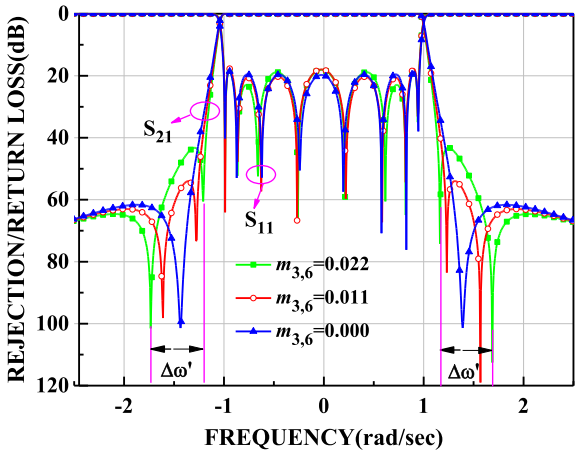

(a)

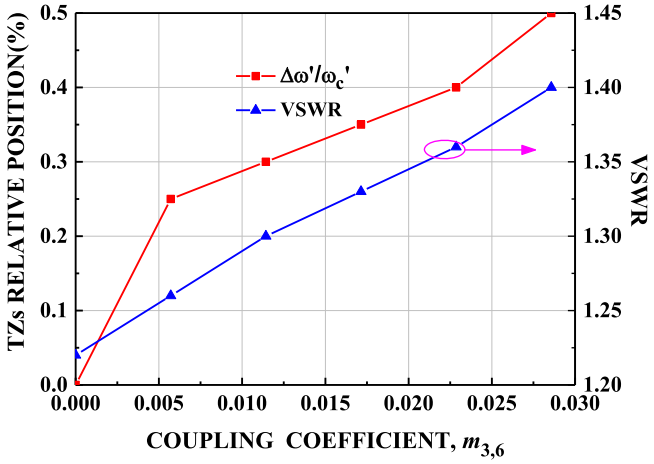

(b)

Figure 7. Analysis of the 8-order symmetrical QCQ filter: (a) frequency response with varied $m_{3,6}$, and (b) the influence of $\Delta\omega'/\omega_c'$ on VSWR.

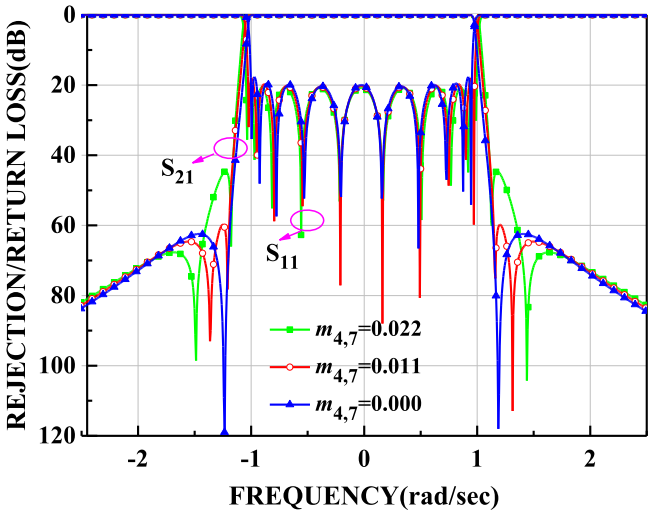

Figure 8. Analysis of symmetrical 10-order QCQ filter in figure 3(a).

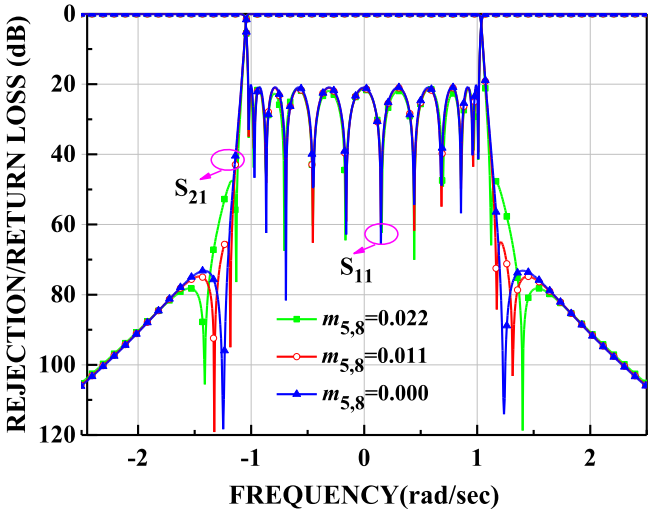

Figure 9. Analysis of symmetrical 12-order QCQ filter in figure 3(b).

3. Analysis of coupling characteristics between resonators

HTS thin film has a very low microwave surface resistance and the filters designed on it possess an extremely high Q value [3, 12–14, 25], so QCQ configuration filters designed by HTS material will possess more obvious TZs and sharper selectivity, and the simulated results will be more approximate to the theoretical ones. The QCQ configuration filter will be constructed by the compact clip-shaped half-wavelength resonator shown in figure 11. This structure is convenient in terms of changing the strength of the main coupling (magnetic field coupling) between two adjacent resonators by adjusting the dimension s, and it is also easy to introduce cross coupling between non-adjacent resonators. The red line in figure 12 shows the phase characteristics (phase of S_{21}) of the main coupling when the distance s between the two resonators is 0.4 mm, and it can be seen that the main coupling property between the two resonators is magnetic field coupling. In addition, the coupling strength decreases with the increase of s, as shown in figure 12. According to the locations of the resonant peaks f_1 and f_2 in figure 12 and equation (1), the non-normalized coupling coefficient $M_{1,2}$ between two resonators can be obtained. Figure 11 shows the coupled resonators' planar structure when the resonant frequency is tuned to 2 GHz.

$$M_{1,2} = \frac{f_2^2 - f_1^2}{f_2^2 + f_1^2} \tag{1}$$

Figure 13 is the CQ unit which can produce a pair of TZs outside the passband. Because the main coupling properties between resonators ① → ②, ② → ③, and ③ → ④ are magnetic field coupling, while the cross coupling between resonators ① → ④ is electric field coupling, there is a phase difference of 180° between the signal paths ① → ② → ③ → ④ and ① → ④, which can create a pair of TZs. Obviously, this unit can also implement the JCC unit.

Figure 14 depicts the relationship between the cross-coupling strength in figure 13 and the locations of TZs. When

Table 3. The normalized coupling coefficient matrix of figure 3(a).

	S	1	2	3	4	5	6	7	8	9	10	L
S	0	0	0	0	0	0	0	0	0	0	0	0
1	0	0	0.780	0	0	0	0	0	0	0	0	0
2	0	0.780	0	0.534	0	−0.165	0	0	0	0	0	0
3	0	0	0.534	0	0.677	0	0	0	0	0	0	0
4	0	0	0	0.677	0	0.474	0	$m_{4,7}$	0	0	0	0
5	0	0	−0.165	0	0.474	0	−0.502	0	0	0	0	0
6	0	0	0	0	0	−0.502	0	0.474	0	−0.165	0	0
7	0	0	0	0	$m_{4,7}$	0	0.474	0	0.677	0	0	0
8	0	0	0	0	0	0	0	0.677	0	0.534	0	0
9	0	0	0	0	0	0	−0.165	0	0.534	0	0.780	0
10	0	0	0	0	0	0	0	0	0	0.780	0	0
L	0	0	0	0	0	0	0	0	0	0	0	0

Table 4. The normalized coupling coefficient matrix of figure 3(b).

	S	1	2	3	4	5	6	7	8	9	10	11	12	L
S	0	0	0	0	0	0	0	0	0	0	0	0	0	0
1	0	0	0.828	0	0	0	0	0	0	0	0	0	0	0
2	0	0.828	0	0.571	0	0	0	0	0	0	0	0	0	0
3	0	0	0.571	0	0.514	0	−0.170	0	0	0	0	0	0	0
4	0	0	0	0.514	0	0.685	0	0	0	0	0	0	0	0
5	0	0	0	0	0.685	0	0.457	0	$m_{5,8}$	0	0	0	0	0
6	0	0	0	−0.170	0	0.457	0	−0.513	0	0	0	0	0	0
7	0	0	0	0	0	0	−0.513	0	0.457	0	−0.170	0	0	0
8	0	0	0	0	0	$m_{5,8}$	0	0.457	0	0.685	0	0	0	0
9	0	0	0	0	0	0	0	0	0.685	0	0.514	0	0	0
10	0	0	0	0	0	0	0	0	−0.170	0.514	0	0.571	0	0
11	0	0	0	0	0	0	0	0	0	0	0.571	0	0.828	0
12	0	0	0	0	0	0	0	0	0	0	0	0.828	0	0
L	0	0	0	0	0	0	0	0	0	0	0	0	0	0

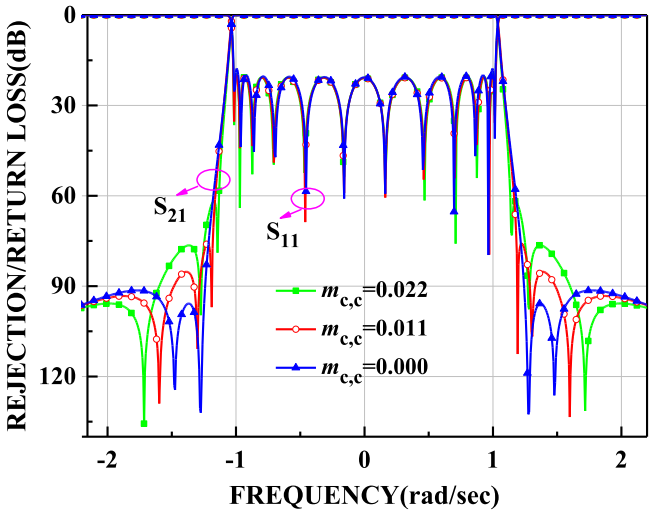

Figure 10. Analysis of symmetrical 12-order QCQ filter in figure 4.

cross coupling is introduced between ① and ④ by the cross-coupling line, TZs can be generated , and as the length t of the cross-coupling line increases from 0 mm to 0.6 mm, as shown in figure 13, the TZs get closer to the center frequency.

4. 8-order symmetrical HTS QCQ configuration filter

Based on the above analysis and multipath coupling diagram of the 8-order QCQ configuration filter in figure 6(a), an 8-order symmetrical HTS QCQ configuration filter is designed on a 0.5 mm thick MgO substrate with double-sided $YBa_2Cu_3O_{7-x}$ films by the full-wave EM simulation software IE3D. According to the normalized coupling coefficient matrix given in table 2, the corresponding coupling coefficients of this filter with the center frequency of 2000 MHz are shown in table 6, and the external quality factor is 53.43. $M_{i,j}$ is the coupling coefficient between resonators i and j, and the minus sign indicates the contrary main coupling property.

Figure 15 shows the layout of the 8-order symmetrical HTS QCQ configuration filter, where the CQ unit in figure 13 is used to construct identical CQ1 and CQ2. The layout in figure 15 is symmetrical about the red dash line. The eight resonators in figure 15 are named ① to ⑧ from left to right, respectively. The CQ unit is constructed by ① → ② → ③ → ④ (⑤ → ⑥ → ⑦ → ⑧), so the two CQ units can produce two pairs of TZs together. And the cross-coupling line between resonator ③ and ⑥ is the introduced JCC, so the JCC unit is constructed by resonators ③, ④, ⑤ and ⑥. By

Table 5. The normalized coupling coefficient matrix of figure 4.

	S	1	2	3	4	5	6	7	8	9	10	11	12	L
S	0	0	0	0	0	0	0	0	0	0	0	0	0	0
1	0	0	0.754	0	−0.262	0	0	0	0	0	0	0	0	0
2	0	0.754	0	0.742	0	0	0	0	0	0	0	0	0	0
3	0	0	0.742	0	0.457	0	$m_{c,c}$	0	0	0	0	0	0	0
4	0	−0.262	0	0.457	0	−0.514	0	0	0	0	0	0	0	0
5	0	0	0	0	−0.514	0	0.508	0	−0.085	0	0	0	0	0
6	0	0	0	$m_{c,c}$	0	0.508	0	0.600	0	0	0	0	0	0
7	0	0	0	0	0	0	0.600	0	0.508	0	$m_{c,c}$	0	0	0
8	0	0	0	0	0	−0.085	0	0.608	0	−0.514	0	0	0	0
9	0	0	0	0	0	0	0	0	−0.514	0	0.457	0	−0.262	0
10	0	0	0	0	0	0	0	$m_{c,c}$	0	0.457	0	0.742	0	0
11	0	0	0	0	0	0	0	0	0	0	0.742	0	0.754	0
12	0	0	0	0	0	0	0	0	0	−0.262	0	0.754	0	0
L	0	0	0	0	0	0	0	0	0	0	0	0	0	0

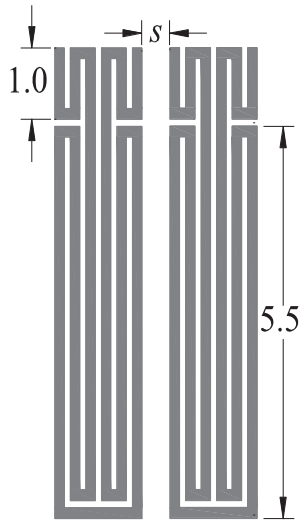

Figure 11. Proposed clip-shaped half-wavelength resonators.

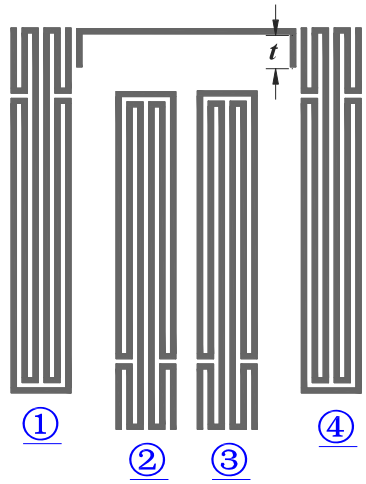

Figure 13. CQ unit with a pair of TZs at finite frequencies.

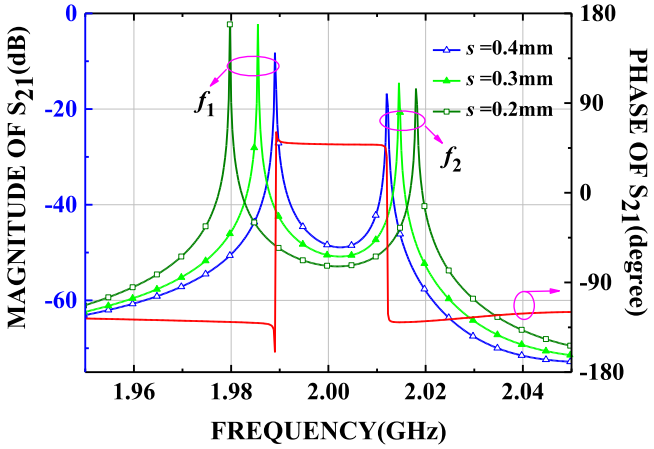

Figure 12. Analyses of coupling phase property and coupling strength.

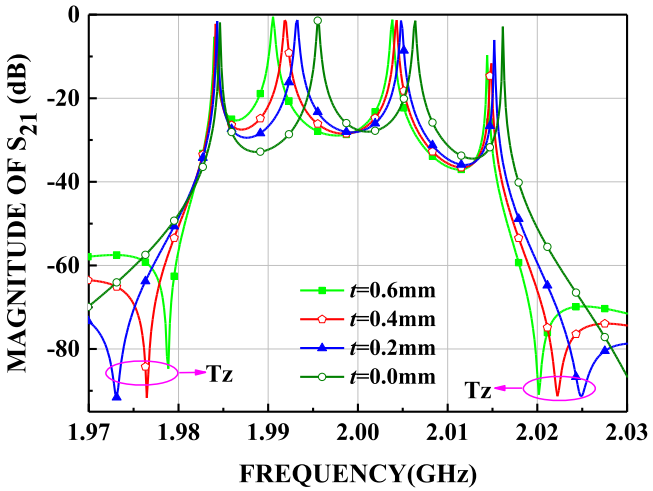

Figure 14. Relationship between the cross-coupling strength and TZs.

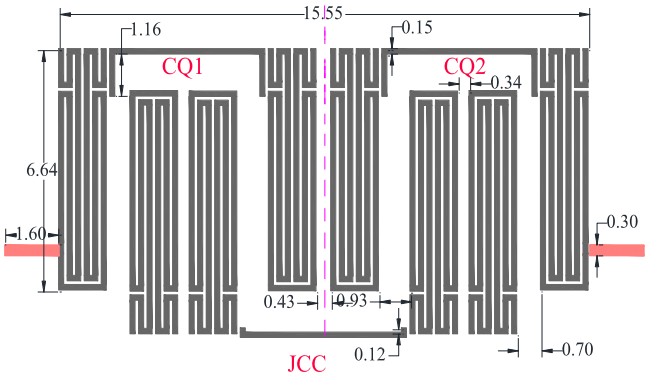

Figure 15. Layout of the 8-order symmetrical HTS QCQ configuration filter.

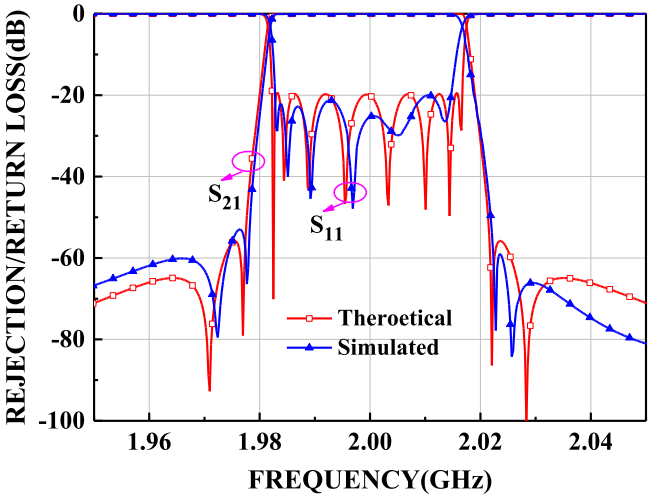

Figure 16. Theoretical and simulated results of the 8-order symmetrical HTS QCQ configuration filter.

Table 6. The coupling coefficients of the 8-order symmetrical HTS QCQ configuration filter.

$M_{1,2} = M_{7,8}$	$M_{2,3} = M_{6,7}$	$M_{3,4} = M_{5,6}$	$M_{4,5}$
0.0133	0.0117	0.0086	0.0090
$M_{1,4} = M_{5,8}$	$M_{3,6}$		
−0.003	−0.0003		

simultaneously adjusting the lengths of the ends of the cross-coupling lines between resonators ① and ④ (resonators ⑤ and ⑧), as shown in figure 15, different coupling strengths are obtained for achieving the coarse tuning of TZs. And by adjusting the lengths of JCC at the ends of the cross-coupling lines between the two same CQ units to get different coupling strengths, the separation of two pairs of TZs and the tuning of their relative distance can be achieved, which means the symmetrical filter can be used to obtain the frequency response of the asymmetrical filter.

Due to the symmetry of the structure, the number of design variables is halved, which can exponentially reduce

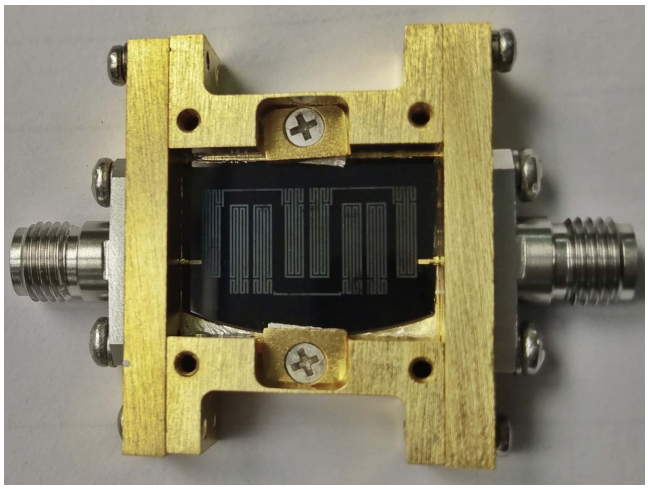

Figure 17. Fabricated 8-order symmetrical HTS QCQ configuration filter.

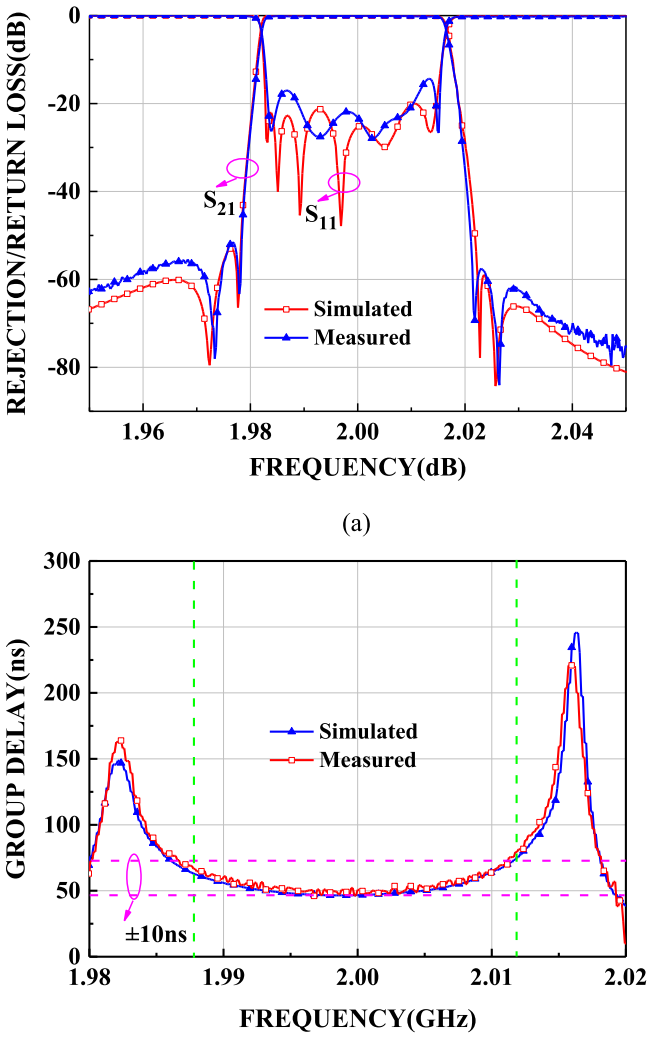

Figure 18. Measured and simulated results of the 8-order symmetrical HTS QCQ configuration filter: (a) S-parameters, (b) group delay.

the design difficulty and time for the frequently-used iterative method of EM simulation. In addition, the more order the filter has, the more effective the method is. Finally, an excellent frequency response is obtained when $M_{3,6}$ is equal to −0.0003. The eventual theoretical and simulated results are shown in figure 16.

Figure 17 is the photograph of the fabricated 8-order symmetrical HTS QCQ configuration filter with a size of 18.75 mm × 7.92 mm, and the widths of line and slot are both 0.15 mm. The filter circuit board is assembled in the metal shielding box made of brass material with good electrical and thermal conductivity, and then the box is fixed on the cold head of the cryocooler in the vacuum chamber. When the test temperature is 77 K, the frequency responses and group delay are measured with the vector network analyzer Agilent E8362B. The measured results of the filter are plotted in figure 18 and agree rather well with the simulated ones. The measured results show that the center frequency is 2000 MHz, the bandwidth 35 MHz, and the group delay fluctuation of less than ±10 ns takes up 70% of the filter's bandwidth. The maximum insertion loss in the passband is 0.16 dB and the reflection in the passband is better than −14.51 dB. There is a slight deviation between the thickness of the actually used superconducting thin film and the simulated one, and there also exists errors in the processing of the circuit. These two main reasons lead to the difference between simulated and measured S_{11} values in figure 18(a).

5. Conclusion

By introducing JCC between two adjacent CQ units in a symmetrical filter, the separation of overlapped TZs and tuning of their relative distance can be realized conveniently. Meanwhile, a series of QCQ configuration filter prototypes and corresponding normalized coupling coefficient matrices are given to facilitate rapid design for designers in the future. An 8-order symmetrical HTS QCQ configuration filter is designed to verify the correctness and feasibility of the proposed method, and the final test results show good agreement with the simulated ones, which shows the proposed QCQ configuration is effective and attractive for TZs adjustment.

ORCID iDs

Liguo Zhou https://orcid.org/0000-0003-0453-9479
Zhihe Long https://orcid.org/0000-0003-3815-2029

References

[1] Ji L Y *et al* 2010 *Sci. Chin. Inf. Sci.* **53** 1903–7
[2] Shaman H and Hong J S 2007 *IEEE Trans. Microw. Theory Tech.* **55** 1780–5
[3] Macchiarella G 2002 *IEEE Trans. Microw. Theory Tech.* **50** 1779–83
[4] Feng C *et al* 2010 *Physica* C **470** 1959–61
[5] Amari S, Rosenberg U and Bornemann J 2002 *IEEE Trans. Microw. Theory Tech.* **50** 1969–78
[6] Zhou J, Lancaster M J and Huang F 2004 *IEEE Trans. Microw. Theory Tech.* **52** 1150–6
[7] Levy R and Petre P 2001 *IEEE MTT-S International Microwave Symp. Digest* vol 3 pp 1467–70
[8] Cameron R J 1999 *IEEE Trans. Microw. Theory Tech.* **47** 433–42
[9] Rosenberg U *et al* 2003 *IEEE Trans. Microw. Theory Tech.* **51** 1735–42
[10] Amari S and Rosenberg U 2004 *IEEE Trans. Microw. Theory Tech.* **52** 721–36
[11] Gajaweera R N and Lind L F 2003 *IEEE Trans. Microw. Theory Tech.* **51** 1578–83
[12] Lamecki A *et al* 2004 *IEEE Microw. Wirel. Components Lett.* **14** 174–6
[13] Li C *et al* 2006 *Supercond. Sci. Technol.* **19** S49
[14] Zhang T *et al* 2015 *Supercond. Sci. Technol.* **28** 105012
[15] Zhang G *et al* 2005 *IEEE Trans. Microw. Theory Tech.* **53** 947–51
[16] Brian Thomas J 2003 *IEEE Trans. Microw. Theory Tech.* **51** 1368–76
[17] Miraftab V and Yu M 2009 *IEEE Trans. Microw. Theory Tech.* **57** 2429–38
[18] Xu Z *et al* 2015 *Supercond. Sci. Technol.* **28** 065016
[19] Zhang T *et al* 2015 *Physica* C **519** 153–8
[20] Cameron R J 2003 *IEEE Trans. Microw. Theory Tech.* **51** 1–10
[21] Zhang T L, Yang K and Zhang Y F 2014 *Chinese Sci. Bull.* **59** 1925–8
[22] Amari S *et al* 2005 *IEEE Trans. Microw. Theory Tech.* **53** 3075–81
[23] Zhang T L *et al* 2007 *Cryogenics* **47** 409–12
[24] Yang Y, Yu M and Wu Q 2016 *IEEE Trans. Microw. Theory Tech.* **64** 4463–72
[25] He Y, Wang G and Sun L 2016 *IEEE Microw. Wirel. Components Lett.* **26** 301–3
[26] Montejo-Garai J R *et al* 2005 *IEEE Trans. Microw. Theory Tech.* **53** 1636–42
[27] Tamiazzo S and MacChiarella G 2015 *IEEE Trans. Microw. Theory Tech.* **63** 3408–15
[28] Yeo K S K *et al* 2001 *IEEE Trans. Microw. Theory Tech.* **49** 321–7
[29] Li F *et al* 2007 *Supercond. Sci. Technol.* **20** 611–5
[30] Hong J S and Lancaster M J 2000 *IEEE Trans. Microw. Theory Tech.* **48** 1098–107
[31] Zhang T *et al* 2013 *IEEE Trans. Appl. Supercond.* **23** 1501805
[32] Tsuzuki G *et al* 2002 *IEEE Trans. Microw. Theory Tech.* **50** 2924–9
[33] Yu T *et al* 2009 *IEEE Trans. Appl. Supercond.* **19** 69–75
[34] Gao L *et al* 2009 *IEEE Trans. Microw. Theory Tech.* **57** 1767–73
[35] Li S *et al* 2007 *IEEE Trans. Microw. Theory Tech.* **55** 754–9
[36] Kuroda A *et al* 2015 *IEEE Trans. Appl. Supercond.* **25** 3–6
[37] Lu J C *et al* 2008 *IEEE Trans. Microw. Theory Tech.* **56** 2101–10
[38] Kuo J T *et al* 2000 *IEEE Microw. Guid. Wave Lett.* **10** 94–5
[39] Hong J *et al* 2000 *IEEE Trans. Microw. Theory Tech.* **48** 1240–6
[40] Cameron R J *et al* 2002 *IEEE Trans. Microw. Theory Tech.* **50** 2862–72
[41] Zhang G *et al* 2006 *IEEE Trans. Microw. Theory Tech.* **54** 559–63
[42] Szydlowski L *et al* 2013 *IEEE Trans. Microw. Theory Tech.* **61** 3601–12
[43] Liao C K, Chi P L and Chang C Y 2007 *IEEE Trans. Microw. Theory Tech.* **55** 147–53
[44] Liu H *et al* 2017 *IEEE Trans. Microw. Theory Tech.* **65** 3813–23